

FIG. 1. (color online) Experimental setup (a) and excitation spectrum (b) for atoms in a tilted periodic potential. The width W is plotted as a function of the drive frequency ν . The resonances correspond to a drastic spreading of the atomic wave packet as a result of modulation-assisted tunneling [21] when $\nu \approx i/j \times \nu_B$, where i, j are integers. The parameters are $F_0 = 0.096(1)mg$, $\Delta F = 0.090(4)mg$, $V = 3.0(3) E_R$, and $\tau = 2$ s. The dashed line is a guide to the eye.

BOs by removing the dipole trap confinement in the vertical direction and by reducing the levitation in 1 ms to cause a force that is a small fraction of the gravitational force mg , for which ν_B is near 100 Hz. An additional harmonic modulation of the levitation gradient then results in an oscillating driving force $F(t) = F_0 + \Delta F \sin(2\pi\nu t + \phi)$, where F_0 is the constant force offset, ΔF is the amplitude of the modulation, ν is the modulation frequency, and ϕ is a phase difference between the BOs and the drive. After a given hold time τ we switch off all optical beams and magnetic fields and take in-situ absorption images after a short delay time of $800\mu s$.

We first determine the excitation spectrum. Fig. 1(b) shows the $1/\sqrt{e}$ -width W of the matter wave after $\tau = 2$ s as a function of ν . A series of narrow resonances at rational multiples of ν_B can clearly be identified. In agreement with recent experiments [20, 21], we attribute these resonances to modulation-enhanced tunneling between lattice sites, leading to dramatic spreading of the atomic wave packet. Tunneling between nearest neighbor lattice sites is enhanced when ν_B is an integer multiple j of ν via a j -phonon process [24], while tunneling between lattice sites i lattice units apart is enhanced when ν is an integer multiple i of ν_B . Even combinations thereof, e.g. $i/j = 2/3$ or $2/5$, are detectable.

We now investigate the dynamics of the wave packet in more detail. For this, we use the resonance with $i = j = 1$ and choose $\nu = \nu_B + \Delta\nu$, where $\Delta\nu$ is the detuning. In Fig. 2(a)-(d) we present absorption images and spatial profiles for the weakly-interacting BEC. The time evolution for the width, shape, and center position of the BEC is dramatic. On resonance ($\Delta\nu = 0$), (c) and (d), the atomic ensemble spreads as it develops pronounced edges. We will see below that the center-of-mass motion depends crucially on the phase ϕ . Off resonance, (a) and (b), for small detuning $\Delta\nu = -1$ Hz, the wave packet exhibits giant oscillatory motion across hundreds of lattice sites that we denote as “super Bloch oscillations” (sBO). Note that, for the parameters used here, the amplitude

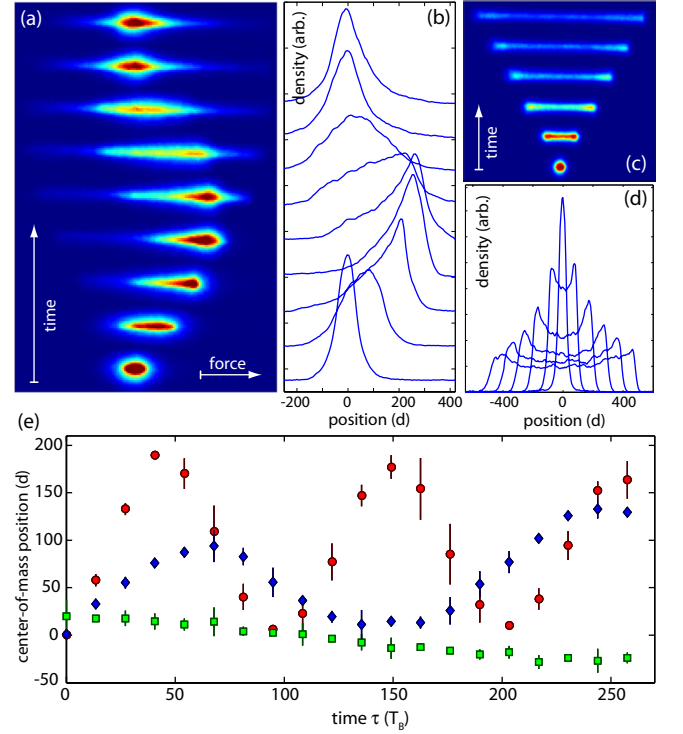


FIG. 2. (color online) Observation of super Bloch oscillations and modulation-driven wave packet spreading. (a) and (b) In-situ absorption images and density profiles for off-resonant modulation ($\Delta\nu = -1$ Hz), showing giant oscillatory motion across more than 200 sites (time steps of 120 ms, average of 4 images). (c) and (d) In-situ absorption images and density profiles for resonant modulation ($\Delta\nu = 0$ Hz), showing a wave packet that spreads symmetrically (time steps of 100 ms, average of 4 images). For (a)-(d), the parameters are $F_0 = 0.062(1)mg$, $\Delta F = 0.092(4)mg$, $V = 3.0(3)E_R$, $a = 11(1) a_0$. (e) Center-of-mass motion for $a = 11(1)a_0$ (squares), $a = 90(1)a_0$ (diamonds), $a = 336(4)a_0$ (squares).

for ordinary BOs corresponds to about $4d = 2.1 \mu m$. Also the width and higher moments of the distribution show oscillatory behavior. In Fig. 2(e) we plot the center-of-mass position as a function of time for $\Delta\nu = -1$ Hz. At $a = 11(1) a_0$ we typically observe sBOs over the course of several seconds. The dynamics of sBOs strongly depends upon the site-to-site phase evolution of the matter-wave. In fact, stronger interactions, e.g. $a = 90(1) a_0$, distort the density profile of the driven BEC and alter the BEC’s oscillation frequency and amplitude. For sufficiently strong interactions, no sBOs are observed. We also attribute the wave-packet spreading as seen after one cycle in Fig. 2(b) mostly to interactions. For the measurements above, we intentionally use a large modulation amplitude ΔF to enhance the amplitude of sBOs. However, all effects equally exist for $\Delta F \ll F_0$, as we will also demonstrate below in Fig. 4(b).

It is useful to develop a simple semi-classical model to obtain a qualitative understanding of the origin of sBOs. The only elements of this model are that the wave packet is accelerated by the applied force and that, once the wave packet